Volume 2, Issue 3
October 2016

AMIC EDUCATIONAL NEWSLETTER

IMAGING THE OBESE PATIENT

Bariatric CT Imaging: Challenges and Solutions

Computed Tomography

By Michael Rogan, M.D.

Over the last 2 decades, there has been an increasing prevalence of obesity among adults in the United States. Obesity is defined as adult body mass index (BMI) > 30, which is weight in kg/height in meters squared. It is projected that by the year 2030 between 42% - 51% of the US population will be obese. In 1990, no state reported an obesity prevalence of more than 14%. In 2008, only one state (Colorado) had an obesity prevalence of less than 20% (Figure 1). In this article, I will describe some of the CT imaging challenges presented by the obese patient, and how those challenges are being solved.

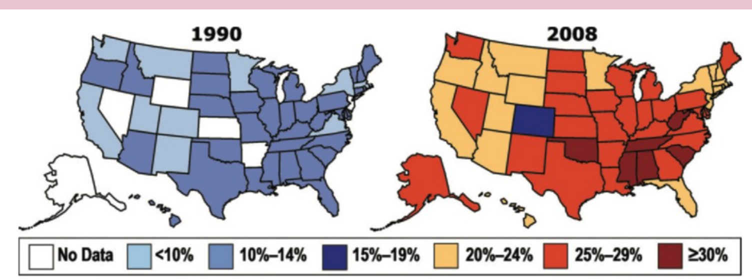

Figure 1: Maps show an increase in the prevalence of obesity in the U.S. adult population between 1990 and 2008. In 1990, no state reported an obesity prevalence of more than 14%. In 2008, only one state (Colorado) had an obesity prevalence of less than 20%.

There are inherent diagnostic limitations related to the physics of CT imaging in the obese patient. Image noise is the most common artifact with obese patient CT images. The CT image is created using the energy photons from the tube source striking a detector after the photons have passed through a person's tissue. Image noise results from insufficient number of photons reaching the detector, due to the greater amount of tissue that inhibits the photons. By increasing the tube current (the mA), this increases the number of photons created, which will reduce noise. When scanning an obese patient, tube current should be the first parameter increased if noise is excessive. Modern CT scanners can produce tube currents in the 800 mA range (Figure 2).

Another option to reduce noise is to increase the time per rotation. This allows more time for photons to penetrate the patient and arrive at the detector. The drawback to this option is that is takes longer to scan the patient, and motion artifacts can occur. Decreasing the pitch (the distance travelled by the scanner in one gantry rotation divided by the beam collimation) to 1 or less results in less noise as well. However, this technique will also increase patient dose and increase scan time.

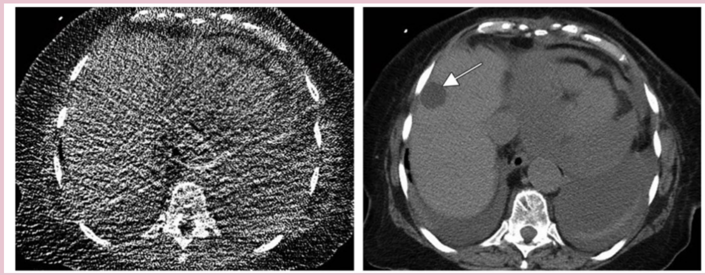

Figure 2: Image (a) was obtained with settings of 130 mAs and 80kVp. Image (b) obtained at 750 mAs and 120 kVp. Notice the reduction in noise artifact in (b) versus (a). The radiation dose to the patient was higher in image (b). The lesion in the liver is identified in image (b) and not identified in image (a).

A third option is to increase the energy of the photons. This is performed when the voltage is increased. Tube voltage (kiloVolts peak, kVp) is the maximum voltage applied across an x-ray. Increasing the voltage results in higher energy photons, which increases the individual photon penetration and decreases noise. Modern CT scanners can produce voltage as high as 140 kVp voltage as high as 140 kVp.

The physical weight needed to be supported by CT scanners has forced industry leaders to change their products. Modern CT scanners now have table loads up to 680 lbs (Figure 3).

Gantry aperture refers to the diameter of the opening in the circular frame housing the tube, the collimating system, and detector array.

Scanner Manufacturer and Model	Aperture Diameter (cm)	Maximum Reconstruction FOV (cm)	Maximum Table Load (lbs)
GE Healthcare			
LightSpeed VCT	70	50	500
LightSpeed Xtra	80	65	650
Philips			
Brilliance CT 64-Channel	70	50	450*
Brilliance CT Big Bore	82	70	650
Siemens			
Somatom Definition AS	78	78	485†
Somatom Sensation Open	82	82	615
Toshiba			
Aquilion 64	72	50	450†
Aquilion Large Bore	90	70	450

Figure 3: Aperture, Field of View (FOV), and Maximum Table Loads for several CT scanners.

Bariatric CT Imaging: Challenges and Solutions

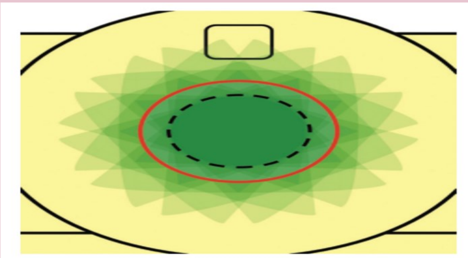

Figure 4: Diagram shows the relation of the scanning FOV (dashed black circle) to the gantry aperture (red circle). The diameter of the scanning FOV is determined by the fan angle of the multiple projections from the x-ray tube and is smaller than the gantry aperture. The reconstruction FOV cannot exceed the scanning FOV.

Gantry aperture refers to the diameter of the opening in the circular frame housing the tube, the collimating system, and detector array.

Older units had an aperture diameter of 70 cm, while newer units have wide gantry diameters of 80 to 85 cm. The scanner field of view (FOV) is always smaller than the gantry aperture because of the fans that the photon source creates. New scanners have a field of view from 50 to 65 cm (Figure 4).

Some common artifacts seen in bariatric imaging are important for the radiologist to be aware of. "Truncation artifact" is an artifact seen when the edge of the image has a high attenuation due to misregistration of the edge of the patient's tissue. For large patients, excess soft tissues may fall outside the scan field of view, but the reconstruction algorithm assumes all the attenuation occurred within the scan field of view. As a result, the edge of the image will have a higher attenuation, which is the truncation artifact. New scanners will have an algorithm that will allow for an expanded field of view option (Figure 5).

Another common artifact is called a "cropping artifact". This artifact occurs when portions of the patient fall outside of the reconstruction field. This may exclude relevant anatomic structures. (Figure 6) .

I hope this article has demonstrated the ways that radiology CT departments have responded to the challenges that obese patients present. Using techniques to increase signal to noise ratio, designing machines with wider gantries and stronger tables, and recognizing different artifacts that obese patients create, the radiology team can maintain high imaging quality for bariatric patients.

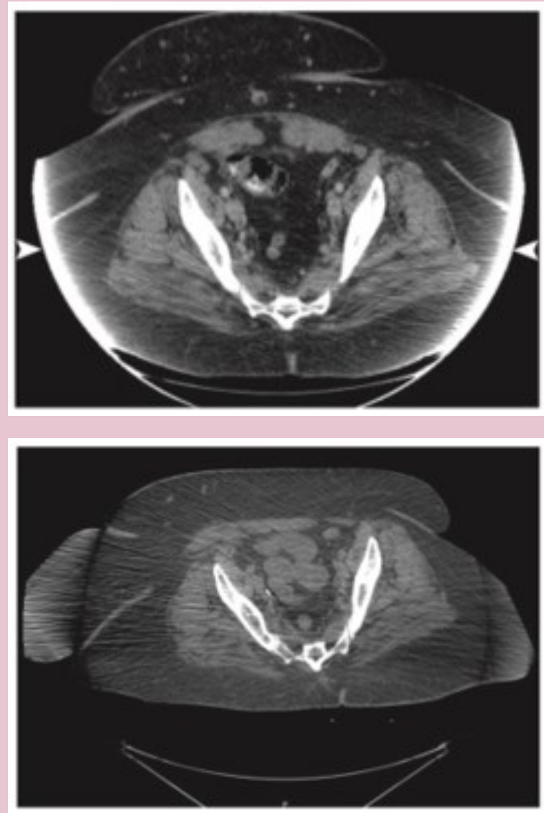

Figure 5: Truncation artifact. The first image shows the flanks extend outside the field of view. The edges of the image show increased attenuation (arrowheads). The second image is obtained in the same patient with a wider FOV, and the truncation artifact is absent.

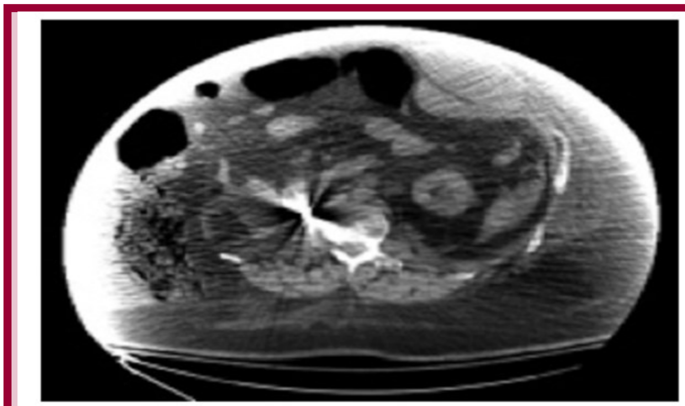

Figure 6: Image obtained for blunt trauma in a patient with BMI of 60. Note the poor depiction of the anterior abdominal wall and the truncation artifact, the high attenuation at the tissue margins.

Michael Rogan, M.D

References:

- Modica, Michael et al. The Obese Emergency Patient: Imaging Challenges and Solutions. Radiographics Volume 31, Issue 3. May-June 2011.

- Dzmitry, Fursevich et al. Bariatric CT Imaging: Challenges and Solutions. Radiographics 2016; 36:1076-1086.

Minimally Invasive Treatment of Varicose Veins

Interventional Radiology

By Winfield M. Craven, M.D.

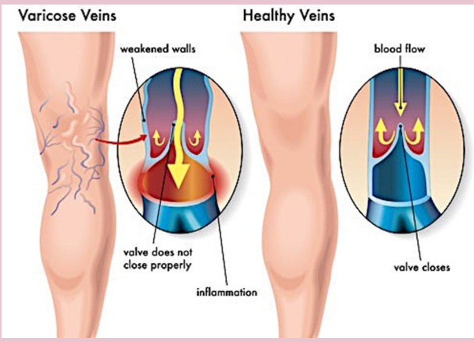

Figure 1: Incompetent valves causing venous insufficiency.

Introduction

Chronic venous insufficiency of the lower extremities is a common benign disease. Up to 25% of adult women and up to 15% of adult man have varicose veins in the distribution of the greater saphenous vein. Risk factors for developing varicose veins include family history, childbearing, sedentary lifestyle, lack of exercise, and obesity. Until recently, the standard treatment of varicose veins was surgical vein stripping. In the last few years, several techniques have been developed for the minimally invasive treatment of varicose veins. The technique used at the Vein and Laser Center of Northern Colorado is endovenous laser treatment (EVLT). Endovenous laser treatment is safe, effective, and less invasive compared to surgery, and it allows patients to return to full activity much quicker. In addition to EVLT, several other procedures are available including microphlebectomies for treatment of varicosities, and ultrasound guided foam sclerotherapy for treatment of incompetent perforating veins.

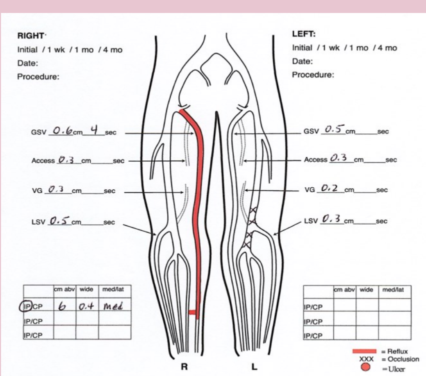

Figure 3: Ultrasound worksheet showing reflux in the right greater saphenous vein, reflux in a right calf incompetent perforating vein, and DVT of the left popliteal vein.

Symptoms

Varicose veins are the result of valvular insufficiency of the superficial venous system. Leaky valves cause backwards venous flow, resulting in enlarged, tortuous superficial varicosities. (Figure 1)

Venous insufficiency can occur throughout the venous system, but occurs most frequently in the great saphenous vein (GSV), lesser saphenous vein (LSV) and other truncal superficial veins. Symptoms of venous insufficiency may include leg heaviness, aching, and restless legs. Symptoms are worsened with prolonged standing and improve with elevation of the legs. Longstanding, chronic superficial venous insufficiency may lead to hyperpigmentation, lipodermatosclerosis, induration, and ulceration.

Evaluation of Venous Reflux

Evaluation of a patient with varicose veins starts with a history and physical examination. The patient then undergoes a venous doppler duplex ultrasound examination. The examination is performed with the patient standing using a rapid cuff inflator (Figure 2).

The cuff is inflated forcing blood out of the leg. An ultrasound transducer is placed on the vein above or below the cuff. The cuff is released and color flow Doppler is used to look for reverse flow in the vein. Reverse flow (reflux) lasting more than 0.5 seconds is considered abnormal. The location and severity of reflux is recorded on an ultrasound worksheet (Figure 3).

Ultrasound Report

Important elements of the ultrasound report include: greatest transverse diameter of the greater, accessory, and lesser saphenous veins, duration of reflux, location of reflux, and location of incompetent perforating veins. The ultrasound examination also includes assessment of the deep venous system looking for thrombosis or reflux.

Contraindications

Absolute contraindications for EVLT include pregnancy, or severe peripheral arterial disease. Relative contraindications include acute DVT, acute superficial thrombophlebitis, or genetic hypercoagulability disorders.

Ideally, anticoagulants need to be withheld for several days prior to EVLT and phlebectomies. Patients who cannot be taken off blood thinners can expect to have more bruising and a higher risk of venous recanalization.

Figure 2: Testing for venous reflux using a rapid cuff inflator.

Conventional Treatment

Conservative treatments such as weight loss, leg elevation, or compression stockings may slow the progression of symptoms, but do not treat the underlying cause of the disease. As a result, varicose veins usually worsen over time. As the disease progresses, legs and feet may begin to swell and sensations of pain, heaviness, burning or tenderness may occur.

The traditional treatment for venous reflux and varicose veins has been surgical vein stripping, usually performed under general anesthesia. Surgical treatments carry the risks of hematoma, infection, scarring, and nerve injury. Other treatments such as high ligation or phlebectomy treat only visible varicosities without addressing the source of the problem. Surgical treatment often results in prolonged recovery times.

Mechanism of Action

The goal of EVLT is to produce a permanent venous closure while at the same time minimizing endoluminal thrombus formation. Endovenous laser treatment delivers highly concentrated laser energy into the vein walls. Typically, the laser wavelength is set at 1470 nm. This wavelength is preferentially absorbed by interstitial water in the venous walls. The resulting thermal injury damages the venous intima and produces inflammatory thickening which eventually leads to a fibrotic obliteration of the venous lumen.

Minimally Invasive Treatment of Varicose Veins cont…

Figure 4: Appearance of right leg before and 4 months after EVLT.

Technique

After a review of the patient's ultrasound findings, the leg is sterilely prepped and draped. A puncture site is chosen usually as low as possible on the calf. The target vein is accessed under direct ultrasound guidance. An .035 J guide wire or glidewire is advanced across the saphenofemoral or saphenopopliteal junction. Next, a 6 FR sheath is inserted. A 600 µm laser fiber is inserted into the sheath and positioned 3 cm inferior to the saphenofemoral or saphenopopliteal junction.

Under US guidance, a foot pump system is used to inject tumescent anesthesia (dilute lidocaine solution) into the peri-venous space along the entire vein. The tumescent solution externally compresses the vein, causing the vein walls to come into contact, promoting a direct transmission of the laser energy to the vein walls. Tumescent solution also increases the distance between the vein and the skin, isolates the laser fiber from the perivenous structures, and prevents skin burns.

The patient is placed in a Trendelenburg position in order to collapse the vein. The laser fiber is activated in the continuous mode and then pulled back at a constant rate. The goal is to deliver energy into the vein walls at a rate of 40-50 joules/cm. Next, the leg is placed in a compression wrap and a Class II compression stocking.

Immediately after the procedure patients walk on a treadmill for 20 minutes, and then are discharged home. Patients take non-steroidal anti-inflammatory drugs (NSAIDs) for one week and wear compression stockings for two weeks. Patients are encouraged to walk at least 4 times per day for 20 minutes for the first week. Patients can begin resuming normal exercise during the second week. Followup ultrasound and clinical examinations are performed at 1 week, 1 month, and 3 months.

Complications

After EVLT, most patients experience moderate pain and bruising along the treated segments. Discomfort and bruising begin to subside at 5-7 days. Most patients are back to full activities at 2 weeks.

Some patients develop an uncomfortable thermal thrombophlebitis along the inner thigh or calf which is treated with NSAIDS and compression stockings. Thermal phlebitis usually resolves within two weeks.

The incidence of DVT after EVLT is about 2%. The risk of DVT is reduced by correct positioning of the fiber tip at a distance of 3 cm from the saphenofemoral junction, to prevent thermal injury of the common femoral vein. Despite this maneuver, occasionally non-occlusive thrombus extends from the saphenous vein into the lumen of the common femoral vein producing a "knuckle thrombus". In most cases, the knuckle thrombus resolves completely within one month without specific treatment.

Other infrequent complications include infection, nerve injury, and skin burns, which occur less than 1% of the time.

Results

After EVLT, most patients have significant improvement in symptoms and a dramatic reduction in visible varicosities (Figure 4). Published studies report venous closure rates of 99-100% at one week, and 94-98% at one year. The majority of recurrences occur within the first 3 months.

In one study, 114 limbs with GSV incompetence were divided them into three groups: 47 limbs received EVLT using the pulsed mode, 33 limbs received EVLT using the continuous mode, and 34 limbs were treated surgically. Quality of life and venous reflux were improved in all groups. At 3 months GSV reflux was abolished in 94% of limbs treated with EVLT, and in 88% of limbs treated with stripping and ligation. Complications rates including hematoma, infection and nerve injury were higher for the surgical group. Return to normal activity and work were quicker after EVLT.

Coexistence of perforator incompetence

Incompetence of the GSV or the LSV may be accompanied by perforator incompetence in the territory of the treated vein, or at a lower level. During EVLT of the GSV, it is often possible to close the perforating vein by extending the laser treatment across the GSV-perforator junction. If the incompetent perforating vein cannot be reached with the laser, the perforator can be treated separately with ultrasound guided foam sclerotherapy.

Conclusion

Minimally invasive treatments of varicose veins have improved significantly in the last decade. EVLT is a safe and very effective technique in the treatment of saphenous vein insufficiency. Compared to surgical vein stripping, EVLT provides significantly decreased post procedure pain, a quicker return to normal activity, and better patient acceptance.

References

- International Journal of Surgery Volume 10, Issue 3, 2012, Pages 134–139. Minimally invasive treatment of varicose veins: Endovenous laser ablation (EVLA).
- flheartlung.com/speciality-services/cardiovascular-services/ultrasound/venous/
- venacure-evlt.com/endovenous-laser-vein-treatment
- coloradoveinandlaser.com
- consultant360.com/content/chronic-venous-disease

Winfield Craven, M.D.

Fatty Liver—A Diagnosis We Make Everyday. How Much Do We Know About It?

Ultrasound, CT and Nuclear Medicine

By Jamie Colonnello, M.D.

The words and the diagnosis of “fatty liver” are written by AMIC technologists and dictated by AMIC radiologists every day of the week. This diagnosis is being made with the help of our technologists in ultrasound, computed tomography and MRI. Occasionally, the diagnosis can be made incidentally on the ventilation portion of a V/Q scan in nuclear medicine. What exactly is “fatty liver” and what is the clinical significance of this diagnosis? Fatty liver is a condition characterized by triglyceride build-up in liver cells (hepatocytes). This is referred to as steatosis.

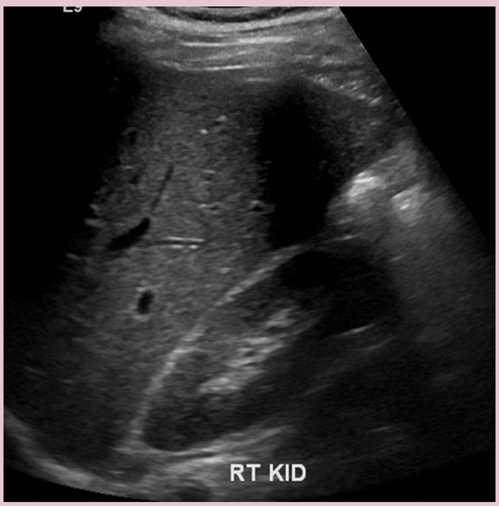

Figure 1: Normal liver echogenicity: isoechoic to slightly hyperechoic to renal cortex.

Fatty liver, or steatosis, can be seen in two subsets of patients. It is commonly seen in patients with alcoholic liver disease. It is seen in 45% of patients who drink greater than 60g of alcohol per day. (For a reference, a can of beer (4-5% ABV) contains approximately 14-15g.) The other, more broad subset of patients fall into the category of non-alcoholic fatty liver disease (NAFLD). This category most commonly is seen in patients with insulin resistance, obesity and hyperlipidemia. Other causes would include viral hepatitis (Hep B and C), drug use (steroids and certain chemotherapy drugs) and congential disorders of metabolism.

In the general population, 15% have fatty liver. If broken down further, it is seen in 50% of patients with hyperlipidemia and 75% of obese patients (BMI >30kg/m2). It is present in 95% of obese patients that drink alcohol regularly.

A small subset of patients with fatty liver will develop associated liver inflammation and this has been termed steatohepatitis (SH). This can be alcohol related but can also non-alcohol related. This entity has been referred to as non-alcohol related SH or NASH. Unfortunately, the mechanism leading to the inflammation is not well understood at this time and it can lead to cell injury, fibrosis/ scarring and cirrhosis.

Treatment for the condition is lifestyle related and starts with minimizing/ eliminating the causative factors. This would include improved diabetes control, decreasing alcohol intake, increasing exercise and diet modification.

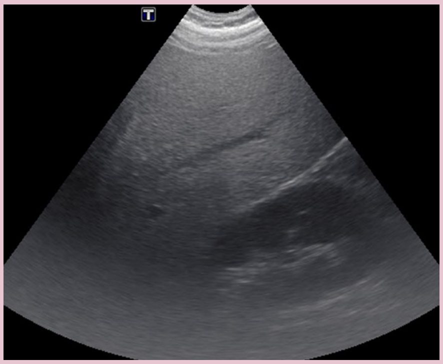

Figure 2: Fatty liver with ultrasound: increase echogenicity of liver compared to renal cortex with poor penetration and with nonvisualiza-

From an imaging standpoint, we can make the diagnosis of fatty liver with multiple modalities. Beginning with ultrasound, normally the liver is isoechoic or slightly hyperechoic compared to renal cortex. (Figure 1). With a fatty liver, the liver is increased in echogenicty when compared to the renal cortex. In addition, the blood vessels in the liver are not well seen and the beam attenuation causes the diaphragm to be ill defined. (Figure 2).

On a noncontrast CT scan, the attenuation of the liver will be slightly greater than that of the spleen. Also, the intrahepatic vessels appear hypoattenuated with respect to the liver. With a fatty liver the converse is seen: the liver is hypoattenuated with respect to the spleen and the vessels appear hyperattenuating. See Figures 3, 4 and 5 to notice this difference.

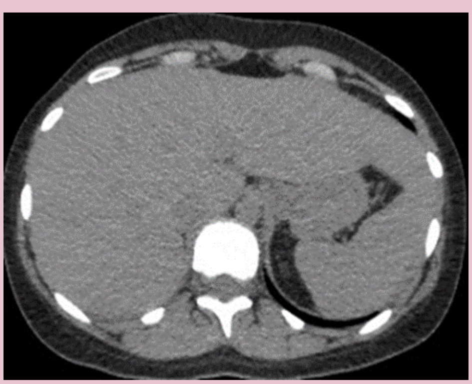

Figure 3: Noncontrast CT image of a normal liver.

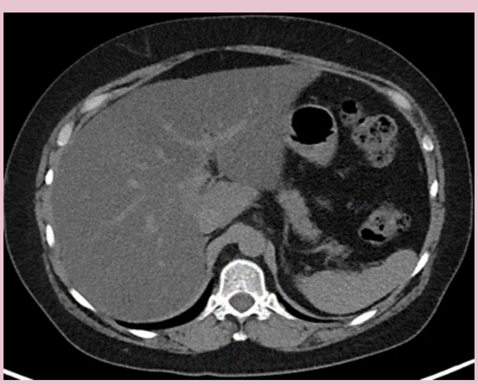

Figure 4: Noncontrast CT of a fatty liver. Note the hyperattenuated vessels and spleen when compared to the

Figure 5: Nonctrast CT of a fatty liver-coronal plane.

Fatty Liver cont…

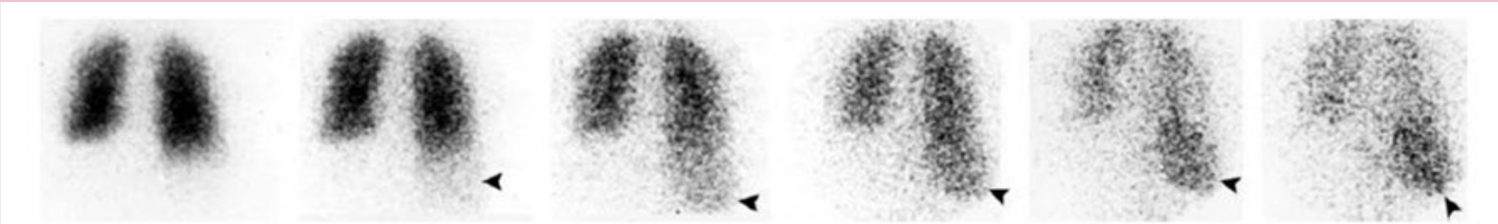

Figure 8: sequential posterior ventilation images from a V/Q scan. Arrow depicts increased Xenon accumulation in a fatty liver below the right lung and diaphragm.

With MRI, the diagnosis can be made with the in and opposed phase T1 weighted sequences. In a normal study, the signal intensity of the liver will remain unchanged between the in and opposed phases. With a fatty liver, there will be loss of signal intensity of the liver on the opposed phase when compared to the in phase. (See and compare Figure 6 and 7.)

Figure 6: in Phase T1 sequence.

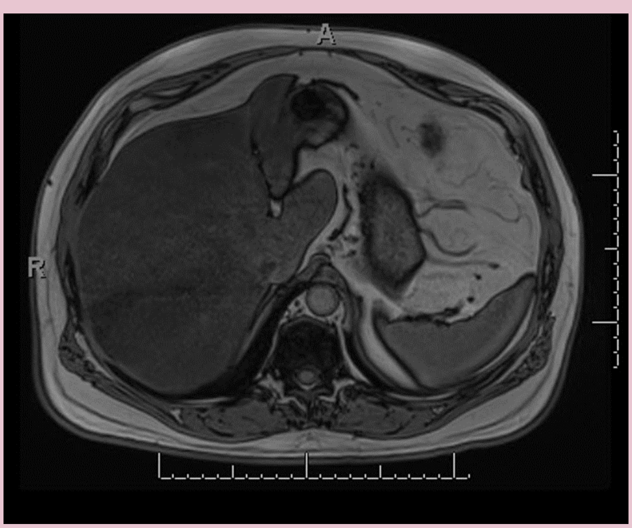

Figure 7: Fatty liver opposed phase T1 sequence. Note the dramatic loss of liver signal compared to the in phase on Figure 6.

Finally, if Xenon-133 is administered to the patient for a ventilation-perfusion nuclear medicine lung scan with fatty liver, there will be a gradual liver uptake noted on sequential ventilation images. Xenon is highly fat soluble and will accumulate and concentrate in fatty tissue. (See figure 8.)

The above imaging examples demonstrate diffuse fatty liver which is the most common appearance with imaging. Other, less common appearances include focal fat deposition or a diffuse pattern with areas of sparing. Areas of sparing commonly are seen with ultrasound near the falciform ligament insertion, along the porta hepatis and along the gallbladder fossa.

To conclude, fatty liver is seen in 15% of the general population and is seen daily in our various imaging locations with multiple imaging modalities. As the obesity epidemic continues in the US, we will undoubtedly see this percentage rise. Hopefully, this review has provided some insight into the meaning of fatty liver while demonstrating the most common appearances with ultrasound, CT, MR and nuclear medicine and raising the awareness of steatohepatitis which can ultimately result in liver cirrhosis.

References

- "Fatty Liver: Imaging Patterns and Pitfalls." Radiographics. Nov-Dec 2006.
- "Xenon 133 Ventilation Studies as an Alternative for Detecting and Quantifying Fatty Infiltration of Liver." Radiographics. Sep-Oct 2009.

Jamie Colonnello, M.D.

Pediatric Liver Lesions

Ultrasound and Computed Tomography

By Kenneth Cicuto, M.D.

Pediatric liver lesions:

Although primary liver lesions are uncommon in the infantile and pediatric population, they are certainly encountered within the busy radiology practice. The liver is the third most common site for infantile intra-abdominal malignancy following the adrenal gland (neuroblastoma) and the kidney (Wilms tumor). Similar to adults, the most common intra-hepatic malignancy is metastatic disease. Primary liver malignancy is rather rare with incidence only approximately 1-1.5 per 1 million in the United States. This figure compromises only a little over 1% of all pediatric primary tumors. Differential considerations or liver masses includes metastases, vascular tumors, primary benign/malignancy liver neoplasms, cysts or abscess. Age of the patient, laboratory findings and imaging characteristics are the best differentiating factors to narrow down the differential.

Presentation:

Fetal and neonatal presentations include hydramnios, fetal hydrops, congestive heart failure or respiratory distress. The vast majority of symptomatic pediatric liver masses will present before the age of 2 with abdominal distention/palpable mass. Ascites and failure to thrive can be more occult presentations in infants. Malignant neoplasms can cause weight loss, fever or anorexia.

Although it is more common to find normal lab results, anemia, thrombocytopenia and leukocytosis can be associated with liver malignancy; alpha fetoprotein (AFP) is the most helpful differentiating lab test for work up evaluation.

Liver neoplasms:

Metastatic disease to the liver is more common than primary neoplasm. The most common primary malignancies include neuroblastoma, Wilms tumor, rhabdomyosarcoma, non-Hodgkin's lymphoma and adrenal cortical carcinoma. Of these cellular origins, neuroblastoma is the most common. Metastatic neuroblastoma can mimic multifocal infantile hemangioendothelioma although the lesions usually enhance LESS than the surrounding liver tissue. Also, adrenal lesions or evidence of retroperitoneal metastases are good clues to this cellular origin. (Figure 1).

Of the primary hepatocellular origin, malignant lesion is twice as common as benign. Of these, hepatoblastoma is the most common. This tumor usually presents before the age of 3 with abdominal mass, anemia, failure to thrive and vomiting. They are commonly associated with elevated AFP and thrombocytosis. These are associated with multiple genetic syndromes/ mutations such as hemihypertrophy, Beckwith-Wiedemann syndrome, polyposis syndromes and trisomy 18.

From an imaging standpoint, these lesion are often large heterogeneous masses within the right lobe with robust arterial enhancement. Intralesional calcifications can be a helpful clue to the correct diagnosis. 10% have pulmonary metastatic disease at the time of diagnosis. AFP is almost always elevated. (Figures 2 and 3).

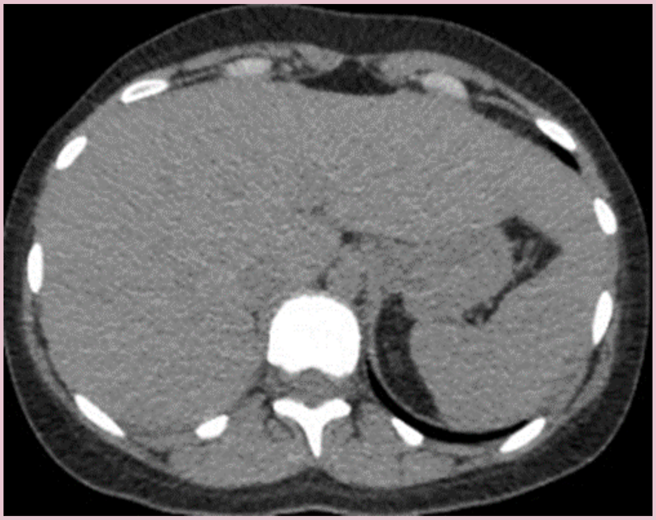

Figure 3

Figure 1

Figure 2

Pediatric Liver Lesions cont…

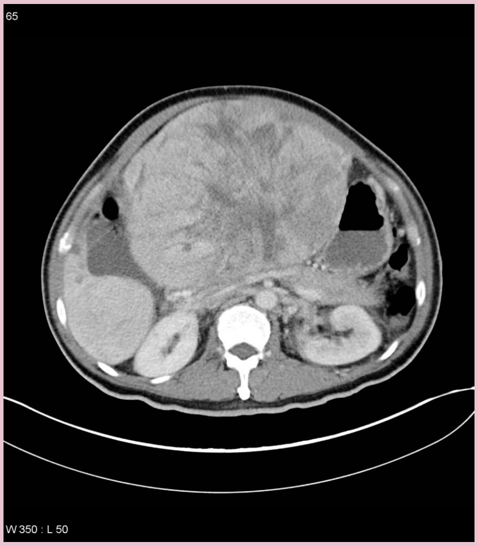

Figure 4

Of the malignant types, hepatocellular carcinoma is the second most common, accounting for one 4th of pediatric hepatic malignancies. for one 4th of pediatric hepatic malignancies. This has a bimodal distribution; presenting ages 0-4 years and ages 10-14 years. Predisposing conditions include hepatic fibrosis and cirrhosis secondary to metabolic liver disease, viral hepatitis, extrahepatic biliary atresia, total parenteral nutrition, and chemotherapy-induced fibrosis.

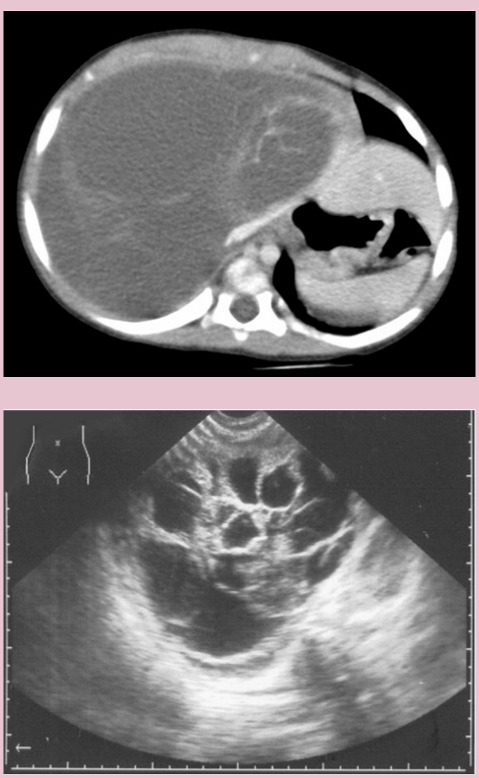

Figure 7

Patients with HCC typically present with abdominal pain caused by the large size of the lesion. Commonly, weight loss, anemia and fever are present. These present as large arterially enhancing lesions with early "washout". Multiple lesions, intravascular spread and metastases are helpful differentiating factors more common in HCC than hepatoblastomas. Similar to hepatoblastoma, the AFP can be elevated. (Figure 4).

Benign lesions:

All site Hemangioendothelioma is the 3rd most common neoplasm is children. Hemangioendotheliomas of the liver is the most common benign hepatic tumor of infancy and is the most common symptomatic tumor prior the age of 6 months. These lesions are rarely discovered after the age of 1 year. Although benign in cellular behavior, serious complications such as high output cardiac failure (AV shunting), platelet sequestration, hypothyroidism and failure to thrive can all occur with these lesions. Imaging wise, these appear as large, high flow lesions with peripheral nodular enhancement central area of necrosis, calcification or fibrosis. 50% are associated with cutaneous hemangiomas. These lesions should regress over time or concern for angiosarcomatous degeneration must be considered. There is no elevation of AFP. (Figures 5 and 6).

Mesenchymal harmartomas are the second most common benign liver mass of childhood. They are composed of myxomatous tissue with malformed bile ducts. In theory, the cause is developmental anomaly of the portal connective tissue. 80 % will present by the second year of life and most common symptom is gradual abdominal distention. They are commonly associated with ascites.

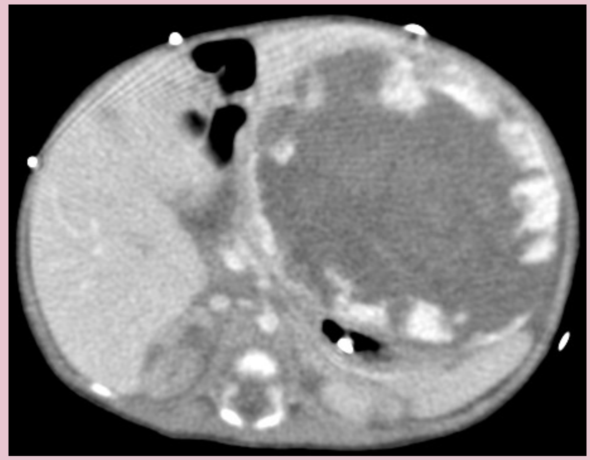

Figure 5

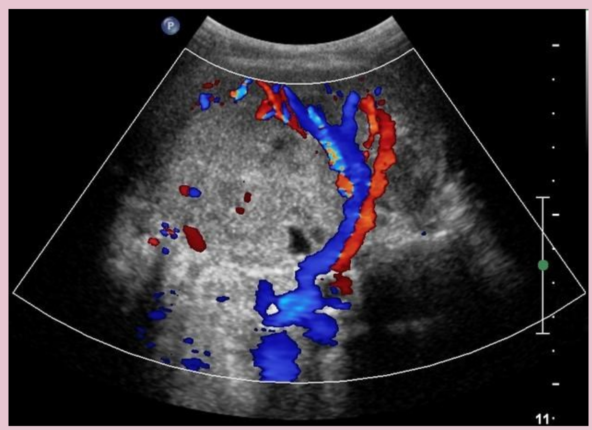

Figure 6

From an imaging standpoint, the major of the lesions are mixed solid and cystic masses within the right hepatic lobe. They are not associated with any specific lab findings. (Figure 7).

Kenneth Cicuto, M.D.

Fluoroscopic Imaging of Bariatric Surgery

Xray
By Amy Hayes M.D.

Bariatric surgery has become increasingly popular in the treatment of obesity. There are two surgical approaches for the treatment of obesity, bypass procedures in which portions of the GI tract are bypassed to cause malabsorption and restrictive procedures in which gastric volume is reduced to induce early satiety. Some of the bypass procedures have been abandoned because of the severe malabsorption in favor of a combination of bypass and restrictive procedures such as the Roux-en-Y gastric bypass. Restrictive procedures including laparoscopic banding and laparoscopic gastric sleeve are the most commonly performed.

Fluoroscopic evaluation is utilized both in the immediate post operative period to evaluate for anastomotic leaks and later to evaluate for complications such as strictures or ulcers.

Roux-en-Y Gastric Bypass

Figure 1 is a pictorial representation of the surgical anatomy. There is creation of a small fundal pouch with Roux Y loop created with a proximal gastrojejunal anastomoses and a distal jejunojenual anastomoses.

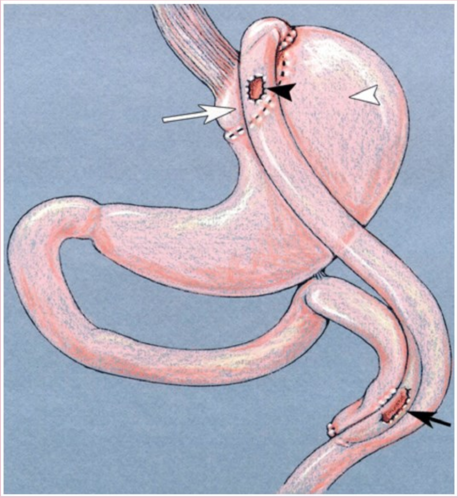

Figure 1: Diagram shows normal surgical anatomy after Roux-en-Y gastric bypass. A staple line partitions the stomach into a small fundal pouch (white arrow) and a much larger excluded stomach (white arrowhead). The jejunal Roux limb is joined proximally to the fundal pouch via a gastrojejunal anastomosis (black arrowhead) and distally to the biliopancreatic limb via a jejunojejunal anastomosis (black arrow). (Reprinted, with permission, from reference 12.)

Normal Fluoroscopic Anatomy

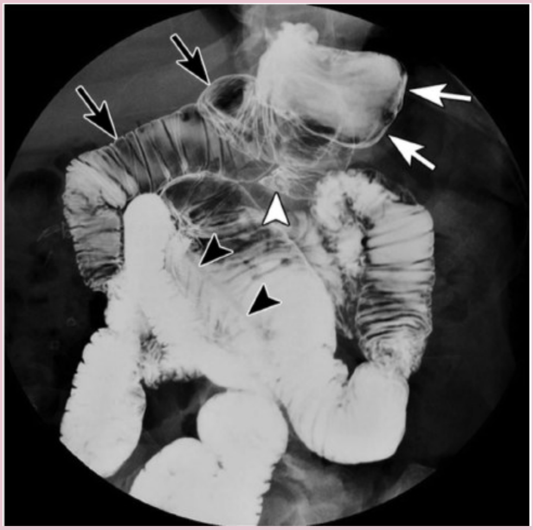

Figure 2: Normal imaging findings after Roux-en-Y gastric bypass. Supine spot image from single-contrast upper GI barium study shows opacified gastric pouch (white arrows), with barium entering Roux limb (black arrows) and blind-ending jejunal stump (white arrowhead). Note widely patent side-to-side jejunojejunostomy (black arrowheads) visualized in profile. Gaseous distention of small bowel loops resulted from aerophagia (not administration of effervescent agent).

Post Operative Leak

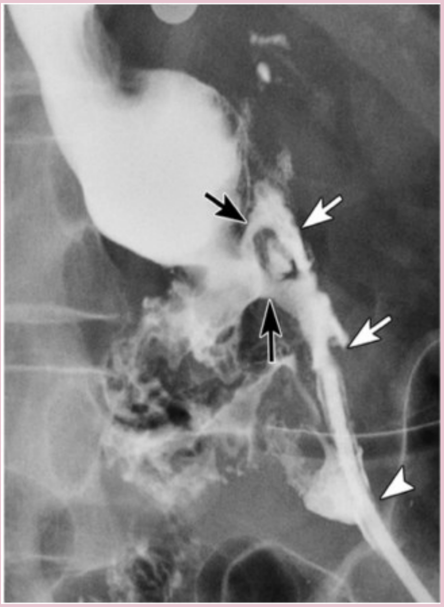

Figure 3: Roux-en-Y gastric bypass with postoperative anastomotic leak. Supine spot image from upper GI examination with water-soluble contrast material shows focal extravasation from left lateral aspect of gastrojejunal anastomosis into two short tracks (black arrows) and adjoining extraluminal collection (white arrows). Note contrast material passing through and around drain (arrowhead) that communicates with inferior aspect of this collection.

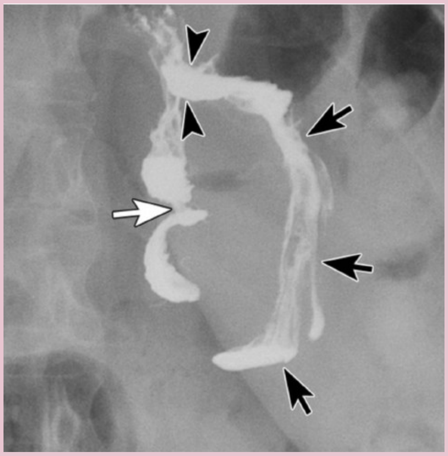

Figure 4: Breakdown of the staple line with passage of contrast into the excluded stomach.

Fluoroscopic Imaging of Bariatric Surgery cont...

Anastamotic Stricture

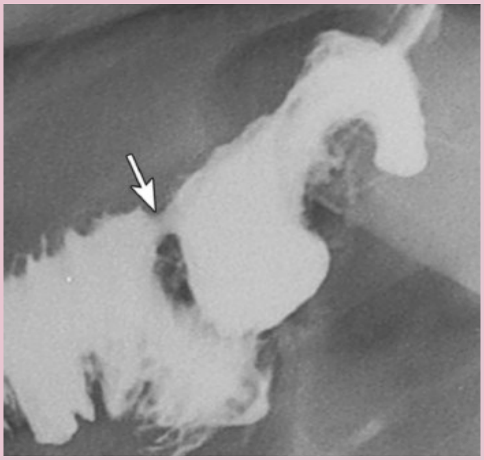

Figure 5: Anastomotic stricture at the gastrojejunal anastomoses (white arrow).

Laparoscopic Band

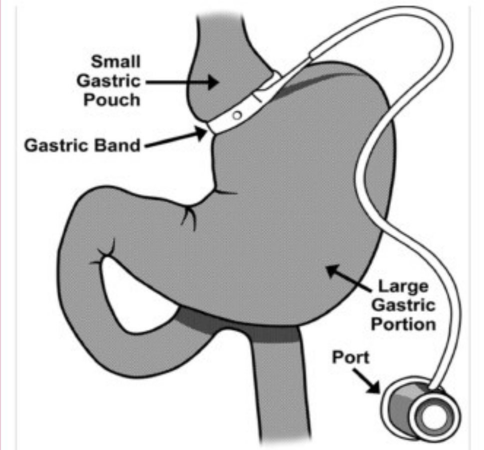

Figure 6: Band is placed laparoscopically approximately 2 cm distal to the GE junction, around the proximal stomach to create a small gastric pouch. Normal orientation of the band can range from 4-58 degrees relative to the spinal column.

Normal Fluoroscopic Appearance

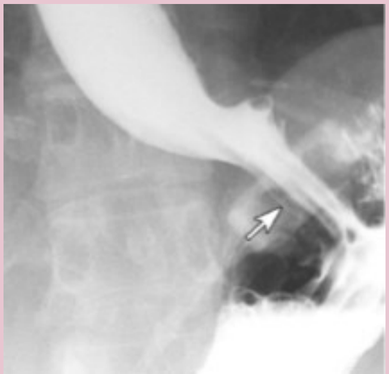

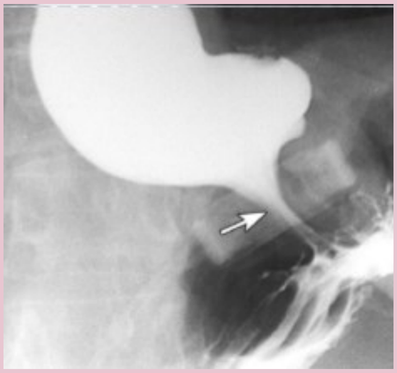

Figure 7: Normal orientation of the band with mild narrowing of the lumen (left) and moderate to severe narrowing (right). Lumen can be adjusted by injecting or withdrawing saline.

Slipped Band

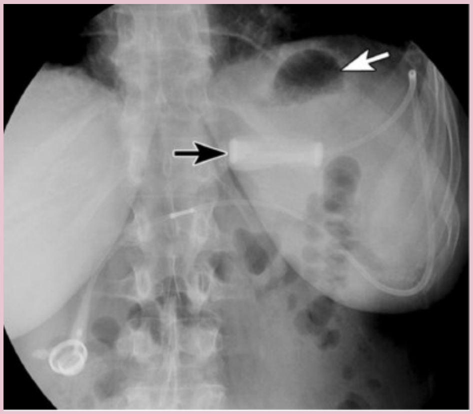

Figure 8: Horizontal orientation of the band secondary to slippage of the band.

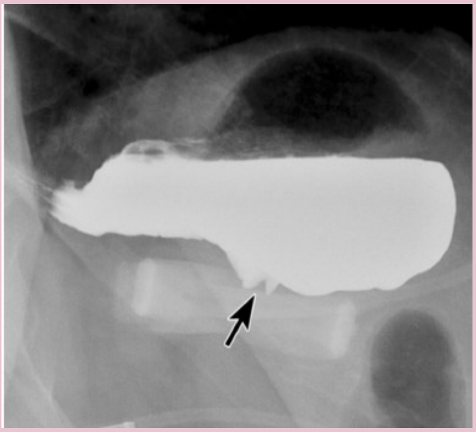

Figure 9: High grade obstruction secondary to slippage of the band.

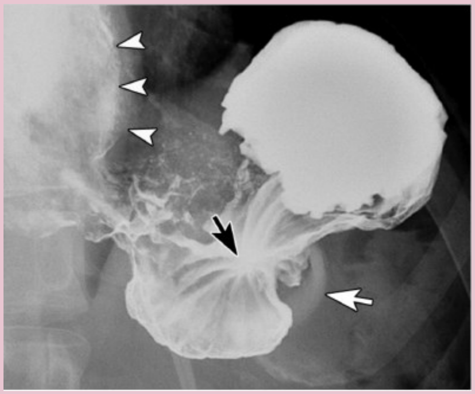

Figure 10: Slippage of the band distally (white arrow) with a gastric volvulous above the band.

Fluoroscopic Imaging of Bariatric Surgery cont...

Laparoscopic Band

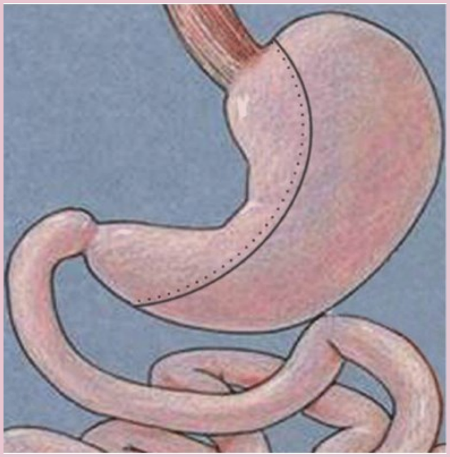

Figure 11: Diagram shows normal surgical anatomy after laparoscopic sleeve gastrectomy. Note how stomach is resected along greater curvature of fundus, body, and proximal antrum, producing a narrow, banana-shaped pouch along lesser curvature.

Normal Postoperative Anatomy

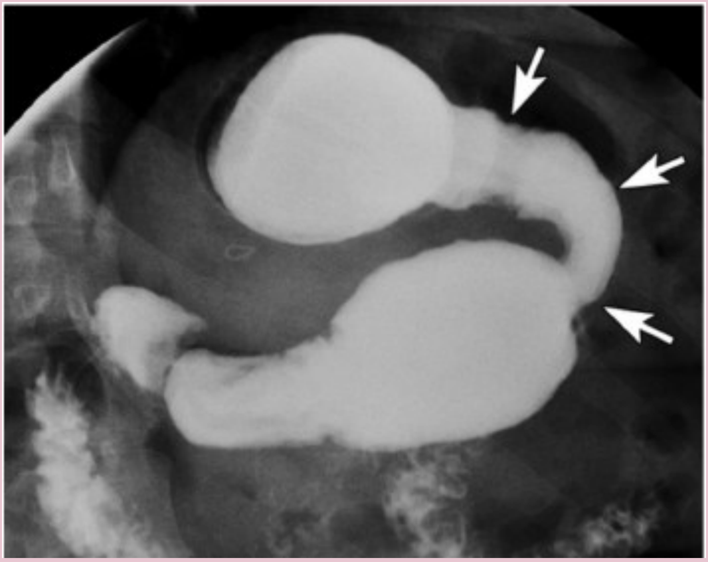

Figure 12: Normal imaging findings after sleeve gastrectomy. Supine spot image from single-contrast upper GI barium study shows tabular narrowing of gastric pouch (arrows) secondary to resection of greater curvature of proximal and mid stomach. Note relatively abrupt widening of gastric antrum, which is preserved.

Post Operative Complications

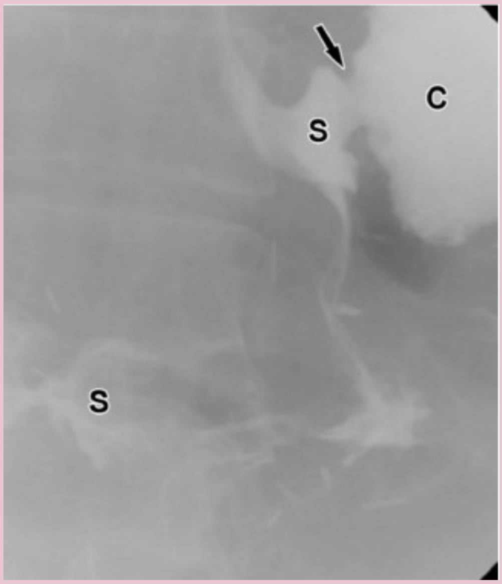

Figure 13: Focal leak from the proximal stomach (arrow) into a left upper quadrant collection (C).

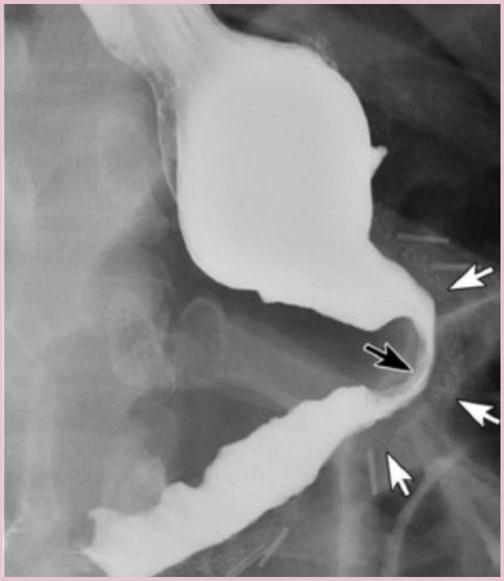

Figure 14: Stricture of the gastric pouch (black arrow). White arrows are the staple line.

Amy Hayes, M.D.

Featured Columnists:

Michael Rogan, MD

Board-Certified: American Board of Radiology

Fellowship/Subspecialty: Body Imaging, University of Vermont College of Medicine, Burling, VT
Interventional Radiology, University of Minnesota, Minneapolis, MN

Residency: Diagnostic Radiology, University of Minnesota Medical School, Minneapolis, MN

MD: University of Minnesota Medical School, Minneapolis, MN

Jamie Colonnello, MD

Board-Certified: American Board of Radiology

Fellowship/Subspecialty: Musculoskeletal Radiology, Washington University—Mallinckrodt Institute of Radiology, St. Louis, MO

Residency: Diagnostic Radiology, Washington University—Mallinckrodt Institute of Radiology, St. Louis, MO

MD: St. Louis University, St. Louis, MO

Winfield Craven, MD

Board-Certified: American Board of Radiology

Fellowship/Subspecialty: Angiography and Interventional Radiology, University of Colorado School of Medicine, Denver, CO

Residency: Diagnostic Radiology, University of Colorado School of Medicine, Denver, CO

MD: University of Cincinnati, Cincinnati, OH

Kenneth Cicuto, MD

Board-Certified: American Board of Radiology

Fellowship/Subspecialty: Vascular and Interventional Radiology, Medical College of Wisconsin, Milwaukee, WI

Residency: Diagnostic Radiology, Maine Medical Center, Portland, ME

MD: St. Louis University School of Medicine, St. Louis, MO

Amy Hayes, MD

Board-Certified: American College of Radiology

Fellowship/Subspecialty: Vascular & Interventional Radiology, University of New Mexico Health Science Center, Albuquerque, NM

Residency: Diagnostic Radiology, Virginia Mason Medical Center, Seattle, WA

MD: University of Massachusetts School of Medicine, Worcester, MA